Proc. Natl. Acad. Sci. USA
Vol. 93, pp. 11950–11955, October 1996
Neurobiology

Targeted deletion of the mouse POU domain gene *Brn-3*a causes a selective loss of neurons in the brainstem and trigeminal ganglion, uncoordinated limb movement, and impaired suckling

MENGQING XIANG*†‡§, LIN GAN§¶, LIJUAN ZHOU*†, WILLIAM H. KLEIN¶‖, AND JEREMY NATHANS*†‖**††

Departments of *Molecular Biology and Genetics, **Neuroscience, and ††Ophthalmology, †Howard Hughes Medical Institute, Johns Hopkins University School of Medicine, Baltimore, MD 21205; and ¶Department of Biochemistry and Molecular Biology, University of Texas M. D. Anderson Cancer Center, Houston, TX 77030

Contributed by Jeremy Nathans, July 30, 1996

ABSTRACT **The *Brn-3* subfamily of POU domain genes are expressed in sensory neurons and in select brainstem nuclei. Earlier work has shown that targeted deletion of the *Brn-3b* and *Brn-3c* genes produce, respectively, defects in the retina and in the inner ear. We show herein that targeted deletion of the *Brn-3a* gene results in defective suckling and in uncoordinated limb and trunk movements, leading to early postnatal death. *Brn-3a* (−/−) mice show a loss of neurons in the trigeminal ganglia, the medial habenula, the red nucleus, and the caudal region of the inferior olivary nucleus but not in the retina and dorsal root ganglia. In the trigeminal and dorsal root ganglia, but not in the retina, there is a marked decrease in the frequency of neurons expressing *Brn-3b* and *Brn-3c*, suggesting that *Brn-3a* positively regulates *Brn-3b* and *Brn-3c* expression in somatosensory neurons. Thus, *Brn-3a* exerts its major developmental effects in somatosensory neurons and in brainstem nuclei involved in motor control. The phenotypes of *Brn-3a*, *Brn-3b,* and *Brn-3c* mutant mice indicate that individual *Brn-3* genes have evolved to control development in the auditory, visual, or somatosensory systems and that despite differences between these systems in transduction mechanisms, sensory organ structures, and central information processing, there may be fundamental homologies in the genetic regulatory events that control their development.**

A central issue in neural development is the manner in which genetic regulatory circuits govern the development of vast numbers of distinct neuronal types. Among the transcriptional regulators implicated in both invertebrate and vertebrate neural development are members of the POU domain family. This family was initially defined by the mammalian pituitary-specific factor Pit-1, the octamer binding factors Oct-1 and Oct-2, and the *Caenorhabditis elegans* gene *Unc-86* (1). The POU domain functions as a bipartite DNA binding domain that contains a ≈70-amino acid POU-specific domain and a ≈60-amino acid POU-homeo domain, joined by a variable linker. The POU domain family has been divided into six classes based on primary sequence similarities in the POU domain (2). Many members of this gene family have distinctive patterns of expression in the developing and adult nervous systems, consistent with a role for these factors in neural development (2).

Genetic and biochemical studies in *C. elegans*, *Drosophila*, mice, and humans have begun to elucidate the roles of several POU domain factors in neurogenesis and neuronal specification. For example, in the neuroendocrine system Pit-1 binds to and activates the growth hormone gene (3, 4), and mutations in *Pit-1* result in dwarfism in both mice and humans secondary to a loss of the growth hormone secreting somatotrophs in the anterior pituitary (5–8). The class III POU domain gene *Brn-4/RHS2* is expressed in the otic vesicle and in other regions in the central nervous system in the developing rat (9, 10), and in humans, mutations in this gene result in stapes fixation and progressive sensorineural deafness (11). Another class III gene, *Brn-2*, is essential for the specification of certain neuronal precursors in the hypothalamus (12, 13).

The class IV POU domain group is defined by the *C. elegans* *Unc-86* gene, the *Drosophila I-POU* gene, and the three vertebrate *Brn-3* genes (14–21). The Unc-86 protein is found exclusively within neurons and neuroblasts, and *Unc-86* loss-of-function mutations alter the fates of a subset of these cells (22, 23). The *Drosophila I-POU* gene encodes both a neuron-specific inhibitor (I-POU) and an activator (tI-POU) that are generated by alternative splicing (15, 16). In mammals, there are three highly homologous class IV POU domain genes, *Brn-3a*, *Brn-3b*, and *Brn-3c* (refs. 17–21; also referred to as *Brn-3.0*, *Brn-3.2*, and *Brn-3.1*, respectively). Each *Brn-3* gene is expressed in a distinct pattern in the developing and adult brainstem, retina, and dorsal root and trigeminal ganglia (17, 19–21, 24, 25). *Brn-3c* is unique among *Brn-3* family members in being expressed in cochlear and vestibular hair cells (ref. 26; M.X. and J.N., unpublished work). The recent production of targeted mutations in *Brn-3b* and *Brn-3c* have revealed a high degree of functional specificity *in vivo*. Targeted deletion of the *Brn-3b* gene results in a selective absence of ≈70% of retinal ganglion cells with little or no effect on other neurons (26, 27), and targeted deletion of *Brn-3c* leads to defective inner ear function as a result of a failure to produce sensory hair cells (26).

During mouse development, *Brn-3a* is expressed in most neurons in the dorsal root and trigeminal ganglia, medial habenula, red nucleus, and inferior olivary nucleus; expression is also seen in scattered neurons in the superior colliculus and periaquaductal grey. In the medial habenula and red nucleus, *Brn-3a* is the only *Brn-3* family member expressed (19–21, 24, 25). In this paper we report the behavioral and neuroanatomic phenotype of targeted deletion of the *Brn-3a* gene.

MATERIALS AND METHODS

Targeted Disruption of the *Brn-3a* Gene. Mouse *Brn-3a* genomic sequences were isolated from a genomic DNA library (strain 129/J) constructed in bacteriophage λ using human *Brn-3a*, *Brn-3b*, and *Brn-3c* POU domain segments as probes (17, 21, 27). To generate the gene targeting construct, the *Kpn*I and *Not*I sites of the 3.0-kb *Brn-3a* *Kpn*I–*Not*I fragment 5′ to the *Brn-3a* gene were converted to *Not*I and *Sal*I sites, respectively, by blunting the ends and adding *Not*I and *Sal*I linkers.

The publication costs of this article were defrayed in part by page charge payment. This article must therefore be hereby marked "*advertisement*" in accordance with 18 U.S.C. §1734 solely to indicate this fact.

Abbreviations: ES, embryonic stem; e, embryonic day; P0, birth.

‡Present address: Center for Advanced Biotechnology and Medicine, Department of Pediatrics, University of Medicine and Dentistry of New Jersey, Robert Wood Johnson Medical School, Piscataway, NJ 08854.
§M.X. and L.G. contributed equally to this work.
‖To whom reprint requests should be addressed.

The *Bst*XI site of the 1.6-kb *Bam*HI–*Bst*XI fragment 3′ to the *Brn-3a* gene was similarly changed to a *Xho*I site. The resulting 3.0-kb *Not*I–*Sal*I 5′ fragment and 1.6-kb *Bam*HI–*Bst*XI fragment were inserted in the correct orientation into the pKO targeting vector (L.G., unpublished results). The targeting construct was linearized at a unique *Not*I site at the edge of the vector and 25 μg of linearized DNA was electroporated into 10^7 AB-1 enbryonic stem (ES) cells that were then selected for resistance to G418 and 1-(2-deoxy-2-fluoro-β-D-arabinofuranosyl)-5-iodouracil. Among 192 ES colonies resistant to G418 and 1-(2-deoxy-2-fluoro-β-D-arabinofuranosyl)-5-iodouracil, 38 contained the expected homologous recombination event as indicated by Southern blot analysis using a flanking probe. Two targeted ES cell clones were injected into C57BL/6J blastocysts to generate chimeric mice, and these were bred to C57BL/6J mice to produce heterozygous and homozygous mice for further analysis. Embryos and mice were genotyped by PCR amplification of genomic DNA.

Histochemistry and Immunohistochemistry. For frozen sections prepared from paraformaldehyde fixed tissue, immunostaining was performed as described (17, 21). The following modifications were applied for frozen sections from unfixed tissue: prior to preincubation with normal serum, the sections were fixed in 4% paraformaldehyde in PBS for 2 h at room temperature, washed several times in PBS, and treated with 100% methanol for 3 min. Anti-Brn-3a, anti-Brn-3b, and anti-Brn-3c antibodies are described in refs. 17 and 21. As described in ref. 21, the polyclonal anti-Brn-3a antibodies used here cross-react with a ubiquitous nuclear antigen in the adult mouse brain; this cross reactivity is absent in the embryonic and neonatal brain as judged by the colocalization of anti-Brn-3a antibody staining (this study) and *Brn-3a* transcripts by *in situ* hybridization (20) and the loss of anti-Brn-3a antibody staining in *Brn-3a* (−/−) animals (this study). Antibodies were obtained from the following sources: anti-calcitonin gene-related peptide, anti-galanin, anti-neuropeptide Y, and anti-substance P (Chemicon); anti-160-kDa neurofilament (NF160; Sigma); anti-Olf1 (28); monoclonal anti-neuron-specific tubulin (TuJ1; ref. 29).

Nonspecific cholinesterase staining was performed as described in ref. 36 using frozen sections cut from paraformaldehyde-fixed tissue.

Histology and Anatomy. Size comparisons of dorsal root and trigeminal ganglia and of the medial habenula were performed with fresh frozen tissue, as this minimizes shrinkage due to fixation.

RESULTS

Behavioral Defects in Brn-3a (−/−) Newborn Mice. To study the function of *Brn-3a in vivo*, mice carrying a *Brn-3a* null mutation were generated by homologous recombination in ES cells (Fig. 1). As expected for a null mutation, anti-Brn-3a immunoreactivity is absent from homozygous mutant animals in all tissues tested, including those where *Brn-3a* is normally expressed (see Figs. 3 *A* and *B*, 4 *G* and *H*, 5 *A* and *B*, 6 *A* and *B*, 7 *A* and *B*, and 8 *A–D*). These and similar immunostaining results obtained using anti-Brn-3b and anti-Brn-3c antibodies and homozygous *Brn-3b* and *Brn-3c* knockout mice (ref. 27; M.X., L.G., W.K., and J.N., unpublished results) confirm that each anti-Brn-3 antiserum recognizes only the Brn-3 protein against which it was raised (21).

Both *Brn-3a* (+/−) and *Brn-3a* (−/−) mice exhibit grossly normal prenatal development as judged by their similarity to the wild type in external appearance and size [Body weight at embryonic day (e) 20: (+/+), 1.19 ± 0.11 g, n = 12; (+/−), 1.19 ± 0.10 g, n = 19; (−/−), 1.18 ± 0.09 g, n = 3. Body weight at birth (P0): (+/+), 1.36 ± 0.14 g, n = 3; (+/−), 1.38 ± 0.05 g, n = 6; (−/−), 1.35 ± 0.11 g, n = 6]. Postnatally, *Brn-3a* (+/−) mice are indistinguishable from the wild type in growth and behavior, and breeding of *Brn-3a* heterozygotes gave a ratio for

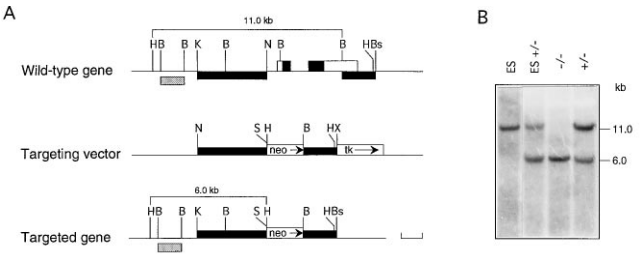

FIG. 1. Targeted deletion of the *Brn-3a* gene. (*A*) Restriction maps of the mouse *Brn-3a* genomic fragment, targeting construct, and targeted *Brn-3a* allele. In the schematic showing the wild-type gene, the two *Brn-3a* exons are shown as boxes above the line, with the open portions representing the 5′ and 3′ noncoding regions and the solid portions representing the protein coding regions. In the targeting vector, a 4.0-kb segment that includes the entire *Brn-3a* coding region was replaced with the PGK-neo cassette (neo) flanked by 3.0 kb of *Brn-3a* 5′ and 1.6 kb of *Brn-3a* 3′ sequences (thick black lines). As seen in the schematic of the targeted gene, the 4.0-kb segment is deleted in the correctly targeted allele. A MC1-herpes simplex virus thymidine kinase cassette (tk) was used for negative selection in 1-(2-deoxy-2-fluoro-β-D-arabinofuranosyl)-5-iodouracil. The orientation of transcription of the PGK-neo and MC1-tk cassettes are shown by arrows. Also indicated are the sizes of the expected wild-type and targeted *Hin*dIII fragments seen after Southern blot hybridization with a 5′ flanking probe (a 2.0-kb *Bam*HI–*Bam*HI fragment; hatched box). Restriction enzymes: B, *Bam*HI; Bs, *Bst*xI; H, *Hin*dIII; K, *Kpn*I; N, *Not*I; S, *Sal*I; X, *Xho*I. Size bracket, 1 kb. (*B*) Southern blot analysis of *Hin*dIII-digested DNA from ES cell lines and from the offspring of a mating between *Brn-3a* (+/−) heterozygotes. The 5′ probe identifies *Hin*dIII fragments of 11.0 kb (wild type) and 6.0 kb (targeted deletion). ES, wild type AB-1 ES cells; ES +/−, targeted ES cells; +/−, *Brn-3a* (+/−) heterozygote; −/−, *Brn-3a* (−/−) homozygote.

all progeny at e20 and P0 of 24:46:24 [(+/+):(+/−):(−/−)], indicating an absence of embryonic lethality associated with deletion of *Brn-3a*.

Unlike their wild-type and heterozygous littermates, *Brn-3a* (−/−) mice do not survive beyond 24 h after birth. Close examination of *Brn-3a* (−/−) neonates revealed two overt behavioral defects. (*i*) *Brn-3a* (−/−) newborn mice do not have visible milk in their stomachs even several hours after birth, suggestive of a defect in suckling (Fig. 2). To specifically examine this, we tested the suckling response in newborn mice by turning them when they were resting and by stimulating their lips with a cannula. None of the six *Brn-3a* (−/−) neonates tested showed evidence of rhythmic jaw opening and closing movements in response to tactile stimulation, whereas each of eight *Brn-3a* (+/+) and 15 *Brn-3a* (+/−) neonates showed a characteristic rhythmic suckling response. *Brn-3a* (−/−) newborn mice remain sensitive to some tactile stimuli, as pinching their limbs causes them to vocalize in a manner

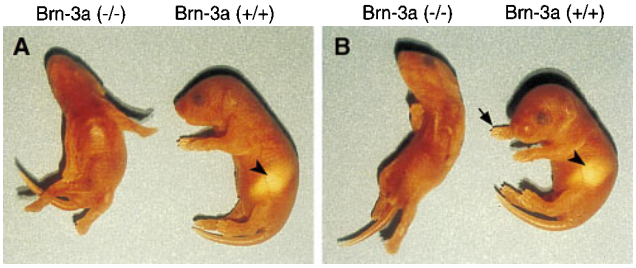

FIG. 2. Behavioral differences between *Brn-3a* (+/+) and *Brn-3a* (−/−) siblings at P0. (*A* and *B*) The *Brn-3a* (+/+) mouse (right) has nursed as seen by the presence of milk in its stomach (arrowhead); the *Brn-3a* (−/−) mouse (left) has not. Both animals were placed on their backs and photographed over the ensuing several minutes. The *Brn-3a* (+/+) mouse uses a forelimb to right itself (arrow in *B*); the *Brn-3a* (−/−) animal extends its limbs, head, and trunk but fails to right itself.

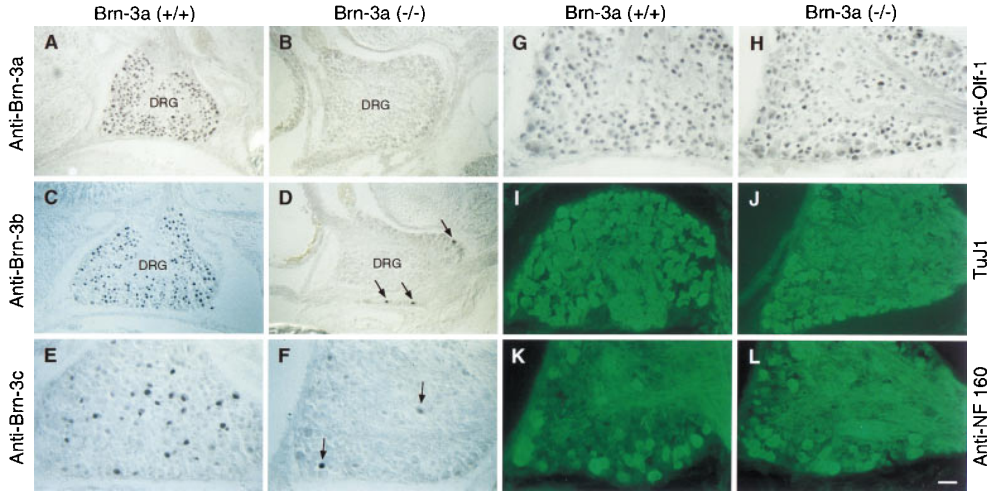

FIG. 3. Dorsal root ganglia in *Brn-3a* (−/−) mice at e20. In each pair of panels in this figure and in Figs. 4–8, *Brn-3a* (+/+) tissue is on the left and *Brn-3a* (−/−) tissue is on the right. In *Brn-3a* (−/−) dorsal root ganglia, Brn-3a immunoreactivity is missing as expected (*A* and *B*) and the number of Brn-3b- and Brn-3c-immunoreactive cells are greatly reduced (*C–F*); the rare Brn-3b- or Brn-3c-immunoreactive cells are indicated by arrows. (*G–L*) The number of cells that are immunoreactive for Olf-1 (*G* and *H*), neuron-specific tubulin (TuJ1) (*I* and *J*), and the 160-kDa subunit of neurofilament (*K* and *L*) are not altered in *Brn-3a* (−/−) dorsal root ganglia. DRG, dorsal root ganglion. (Bars: *A–D*, 50 μm; *E–L*, 25 μm.)

indistinguishable from the wild type. (*ii*) *Brn-3a* (−/−) mice show a deficiency in righting due to a lack of coordinated limb and trunk movements. When a *Brn-3a* (−/−) neonate is placed on its back or side, it typically moves and stretches its limbs ineffectually and displays extended postures not observed in the wild type (Fig. 2). By contrast, *Brn-3a* (+/+) and (+/−) neonates invariably succeed in righting themselves, typically by using the forelimb closest to the ground [Fig. 2*B*; successful righting: (+/+), 100%, $n = 17$; (+/−), 100%, $n = 35$; (−/−), 0%, $n = 23$]. Failure to feed does not appear to be the cause of this righting defect because wild-type siblings that are not allowed to feed retain the ability to right themselves.

In wild-type mice, *Brn-3a* is expressed during development and in the adult in most, if not all, neurons in the trigeminal and dorsal root ganglia, in ≈70% of retinal ganglion cells, and in several brainstem nuclei (19–21, 24, 25). As described below, we have examined the *Brn-3a* (−/−) nervous system in the late gestational and neonatal periods (e20 and P0, respectively) using a combination of histochemistry and immunohistochemistry. This analysis has revealed developmental anomalies in several central nervous system and peripheral nervous system structures that plausibly account for the behavioral defects.

Dorsal Root Ganglia, Trigeminal Ganglia, and Retina. As an initial step in the analysis of the retina and sensory ganglia in *Brn-3a* (−/−) mice, dorsal root ganglia were examined by cresyl violet staining of four *Brn-3a* (+/+) or (+/−) and four *Brn-3a* (−/−) e20 embryos and one pair of *Brn-3a* (+/−) and (−/−) neonates (Fig. 3). Retinas from three *Brn-3a* (+/+) or

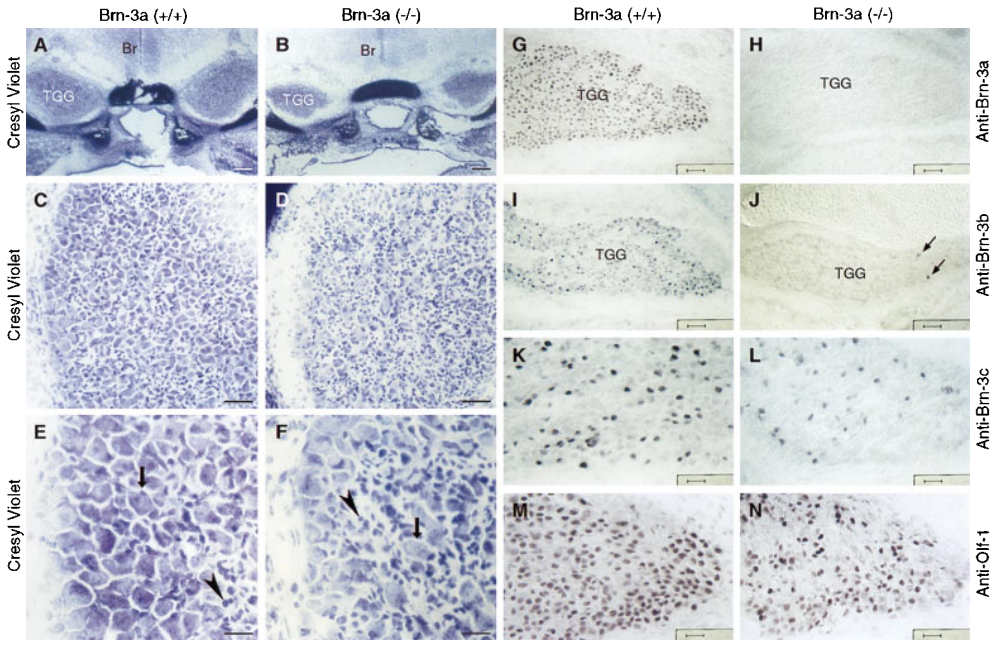

FIG. 4. Trigeminal ganglia in *Brn-3a* (−/−) mice at e20. (*A–F*) Cresyl violet staining shows a 2-fold reduction in size of the *Brn-3a* (−/−) trigeminal ganglia (*A* and *B*) and a selective loss of large cells (*C–F*). (*E* and *F*) Large vertical arrows, large cells; arrowheads, small cells. In *Brn-3a* (−/−) trigeminal ganglia, Brn-3a immunoreactivity is absent as expected (*G* and *H*), the density of Brn-3b-immunoreactive cells is greatly reduced (*I* and *J*) (the rare Brn-3b-immunoreactive cells are indicated by small arrows), the density of Brn-3c-immunoreactive cells is reduced approximately 5-fold (*K* and *L*), and the density of Olf-1 immunoreactive cells is reduced less than 2-fold (*M* and *N*). TGG, trigeminal ganglion; Br, brain. (Bars: *A* and *B*, 200 μm; *C, D*, and *G–J*, 50 μm; *E, F*, and *K–N*, 25 μm.)

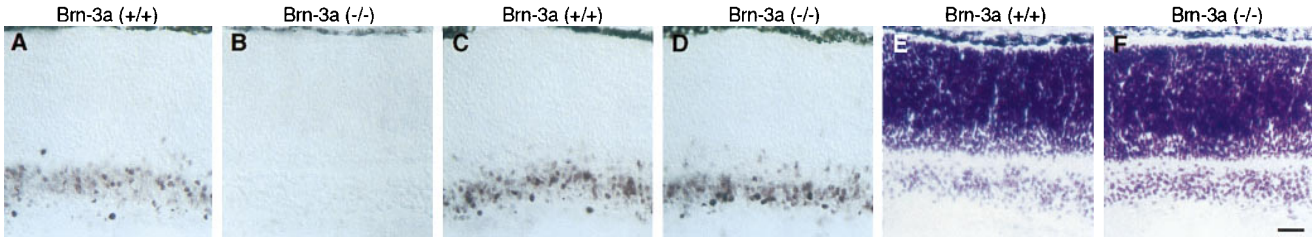

FIG. 5. Retinal structure in *Brn-3a* (−/−) mice at e20. The photographs are aligned with the pigment epithelium at the top and the vitreal surface at the bottom. At this stage the retina consists of a broad zone of mitotic cells and developing neuroblasts in the outer two-thirds of the retina and a ganglion cell layer in the inner one-third. In *Brn-3a* (+/+) retinas, Brn-3a (*A*) and Brn-3b (*C*) immunoreactivity are found only in ganglion cells as reported previously (17, 19–21). In *Brn-3a* (−/−) retinas, Brn-3a immunoreactivity is absent as expected (*B*), and Brn-3b immunoreactivity is unaffected (*D*). In *Brn-3a* (−/−) mice, no differences in retinal structure are discernible by cresyl violet staining (*E* and *F*). (Bars = 25 μm.)

(+/−) and three *Brn-3a* (−/−) e20 embryos and from one pair of *Brn-3a* (+/−) and (−/−) neonates, and trigeminal ganglia from three *Brn-3a* (+/+) or (+/−) and three *Brn-3a* (−/−) e20 embryos were similarly examined (Figs. 4 and 5). While the sizes of the developing retina and dorsal root ganglia, the number of cells within them, and their appearance in the light microscope show no significant differences between *Brn-3a* (+/+) or (+/−) and *Brn-3a* (−/−) mice, the volumes of the trigeminal ganglia of *Brn-3a* (−/−) mice at e20 are approximately one-half that of *Brn3a* (+/+) or (+/−) mice (indistinguisable rostrocaudal lengths and a ratio of coronal cross-sectional areas of 0.58 ± 0.12, $n = 4$; Fig. 4 *A* and *B*). Moreover, *Brn-3a* (−/−) trigeminal ganglia show a significant decrease in the density of large neurons with an accompanying increase in the density of smaller cells compared with *Brn-3a* (+/+) and (+/−) trigeminal ganglia (Fig. 4 *C–F*).

The dorsal root and trigeminal ganglia were further characterized by immunostaining of e20 embryos with a series of antibodies specific for neurons or neuronal subsets. Antibodies against the Olf-1 transcription factor (anti-Olf-1; ref. 28), and the neuron-specific class III β-tubulin (mAb TuJ1; ref. 29) immunolabel the vast majority of neurons in both the dorsal root and trigeminal ganglia of e20 *Brn-3a* (+/+) embryos (Figs. 3 *G* and *I* and 4*M* and data not shown), while anti-neurofilament 160 (anti-NF 160) antibodies stain only a minority of neurons within these two ganglia (Fig. 3*K* and data not shown). Consistent with the cresyl violet staining, there is no significant difference between *Brn-3a* (+/+) and (−/−) animals in the appearance or number of dorsal root ganglion cells that immunostain with anti-Olf1, TuJ1, or anti-NF 160 (Fig. 3 *G–L*). Immunostaining for substance P, galanin, neuropeptide Y, and calcitonin gene-related peptide also reveals equal numbers of immunoreactive neurons in *Brn-3a* (+/+) and *Brn-3a* (−/−) dorsal root ganglia (data not shown). In the trigeminal ganglia, the density of neurons that are Olf-1 immunoreactive show a modest decrease in e20 *Brn-3a* (−/−) embryos as compared with the wild type (Fig. 4 *M* and *N*). Visualization of encapsulated nerve endings in the skin and at the base of hair follicles using nonspecific choline esterase histochemistry (30, 31) did not reveal an alteration in the density of this class of mechanoreceptors in *Brn-3a* (−/−) mice in either the face or the trunk (data not shown).

The other two members of the *Brn-3* family, *Brn-3b* and *Brn-3c*, are expressed in subsets of neurons in the dorsal root and trigeminal ganglia and in subsets of ganglion cells in the retina. Within each of these populations, *Brn-3b* is expressed in a majority of neurons and *Brn-3c* in a minority of neurons (Figs. 3 *C* and *E* and 4 *I* and *K*). Interestingly, Brn-3b-immunoreactive cells are nearly absent in the trigeminal and dorsal root ganglia of *Brn-3a* (−/−) mice (Figs. 3 *C* and *D* and 4 *I* and *J*), and Brn-3c-immunoreactive cells are diminished in number by 5- to 10-fold (Figs. 3 *E* and *F* and 4 *K* and *L*). By contrast, the number and appearance of Brn-3b- and Brn-3c-immunoreactive cells in the e20 retina are unaffected by loss of *Brn-3a* (Fig. 5 *C* and *D*; and data not shown).

Brainstem. Loss of *Brn-3a* affects neither the superficial appearance nor the size of the brain at e20 or P0. To search for defects in the *Brn-3a* (−/−) brain, a complete series of 20-μm coronal sections was prepared from four pairs of e20 *Brn-3a* (+/+) or (+/−) and *Brn-3a* (−/−) brains, and one pair of P0 *Brn-3a* (+/−) and *Brn-3a* (−/−) brains.

In the rostral brainstem, *Brn-3a* expression has been localized by *in situ* hybridization to the habenula in the developing and adult rat brain, and *Brn-3a* is the only *Brn-3* family member expressed in this nucleus (20). At e20 in the mouse, Brn-3a immunoreactivity is present in most neurons in the medial

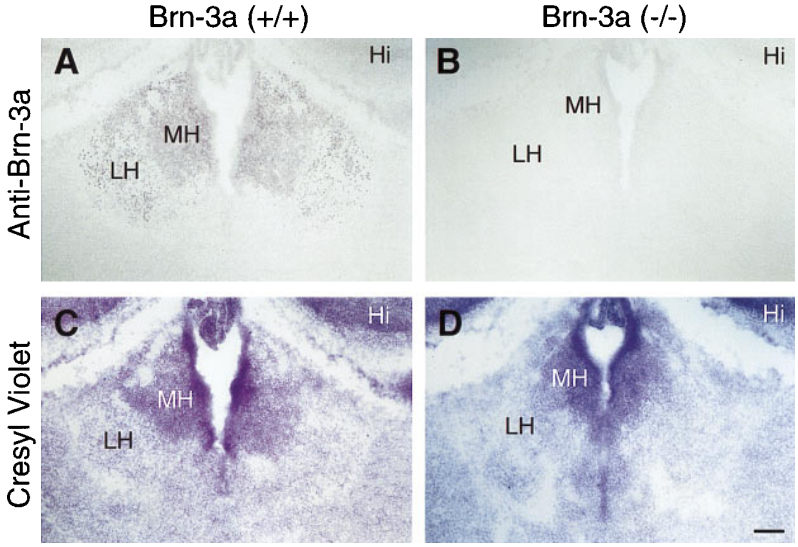

FIG. 6. Habenula in *Brn-3a* (−/−) mice at e20. The coronal sections chosen show the medial habenula at the point of its greatest lateral extent. The dorsal third ventricle is seen at the center of each section. In *Brn-3a* (+/+) mice, Brn-3a-immunoreactive neurons are present at high density in the medial habenula and at lower density in the lateral habenula (*A*). In *Brn-3a* (−/−) mice, Brn-3a immunoreactivity is absent as expected (*B*). Cresyl violet staining shows a loss of neurons in the medial habenula in *Brn-3a* (−/−) mice (*C* and *D*). MH, medial habenula; LH, lateral habenula; Hi, hippocampus. (Bars = 100 μm.)

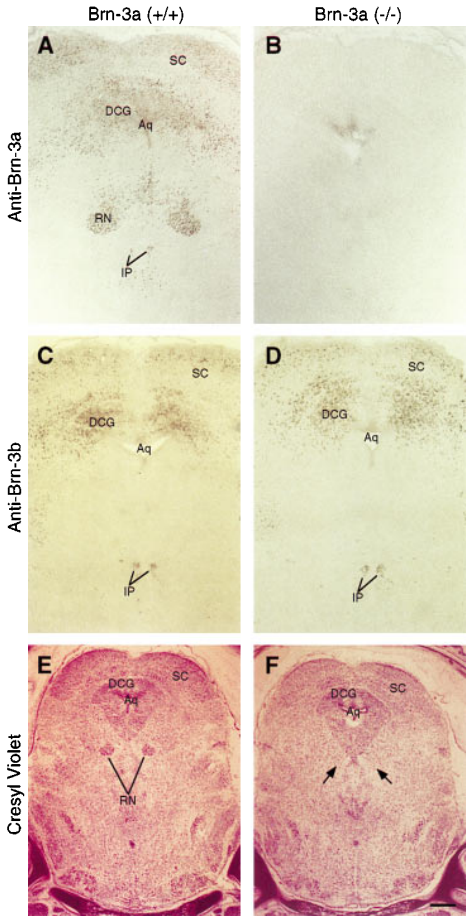

FIG. 7. Midbrain at the level of the red nucleus in *Brn-3a* (−/−) mice at e20. In *Brn-3a* (+/+) mice, Brn-3a-immunoreactive neurons are present in the superior colliculus, dorsal central grey, red nucleus, and the interpeduncular nucleus (*A*); Brn-3b-immunoreactive neurons are present in the superior colliculus, dorsal central grey, and the interpeduncular nucleus (*C*). In *Brn-3a* (−/−) mice, Brn-3a immunoreactivity is absent as expected (*B*), and Brn-3b immunoreactivity is unchanged (*D*). By cresyl violet staining, the large neurons of the red nucleus are absent (*E* and *F*) (arrows in *F* indicate the expected location of the red nucleus). Aq, aquaduct; DCG, dorsal central grey; IP, interpeduncular nucleus; RN, red nucleus; SC, superior colliculus. (Bars: *A–D*, 200 μm; *E* and *F*, 400 μm.)

habenula and in scattered neurons in the lateral habenula (Fig. 6*A*). At this stage, cresyl violet staining shows a reduction of approximately 2-fold in the number of cells in the medial habenula in *Brn-3a* (−/−) mice in comparison with the wild type (Fig. 6 *C* and *D*).

In the midbrain, *Brn-3a* is expressed during development and in the adult in the superior colliculus, dorsal central gray, red nucleus, and interpeduncular nucleus (Fig. 7*A*). With the exception of the red nucleus, *Brn-3b* is also expressed in each of these regions (Fig. 7*C*). No differences are observed between *Brn-3a* (+/+) or (+/−) and *Brn-3a* (−/−) mice at e20 in the number of neurons or in the numbers and locations of Brn-3b-immunoreactive neurons within the superior colliculus, dorsal central gray, or interpeduncular nucleus (Fig. 7 *C–F* and data not shown). By contrast, the large neurons of the red nucleus that are clearly seen in wild-type mice as two symmetric clusters by cresyl violet staining are not seen in *Brn-3a* (−/−) mice at e20 and P0 (Fig. 7 *E* and *F*).

In the inferior olivary nucleus, both *Brn-3a* and *Brn-3b* are expressed during development, but only *Brn-3a* expression persists in the adult (17, 20, 25). At e20, strong Brn-3a immunoreactivity is uniformly present in many neurons in the inferior olivary nucleus along its entire rostrocaudal extent (Fig. 8 *A* and *C*). At this stage, strong Brn-3b immunoreactivity is also present in many neurons in the rostral region of the inferior olivary nucleus, but in the caudal region strong Brn-3b immunoreactivity is confined to the ventral part of the nucleus (Fig. 8 *E* and *G*). Little or no difference is seen between *Brn-3a* (+/+) and *Brn-3a* (−/−) mice in the density or location of cells that are stained by anti-Brn-3b antibodies or by cresyl violet in the rostral region of the inferior olivary nucleus (compare Fig. 8 *E* and *F* with *I* and *J*). However, cresyl violet staining reveals a reproducible diminution in the number of cells in the caudal region of the inferior olivary nucleus in *Brn-3a* (−/−) mice (Fig. 8 *K* and *L*) with little accompanying change in the number of cells that are strongly immunoreactive for Brn-3b (Fig. 8 *G* and *H*).

DISCUSSION

Specificity of *Brn-3a* Function. In this paper we report the behavioral and anatomic phenotypes associated with targeted deletion of the *Brn-3a* gene. Newborn *Brn-3a* (−/−) mice exhibit aberrant limb and trunk movements and impaired suckling, and they die within 1 day. *Brn-3a* (−/−) mice have a decrease in the number of neurons in the trigeminal ganglion, medial habenula, red nucleus, and inferior olivary nucleus and a decrease in the fraction of neurons in the trigeminal and dorsal root ganglia that express *Brn-3b* and *Brn-3c*. Other regions within the nervous system, including those that normally express *Brn-3a*, are not detectably affected.

The behavioral defects seen in *Brn-3a* (−/−) mice could arise from somatosensory dysfunction, motor dysfunction, or a combination of the two. While the observed anatomic defects do not unequivocally define the sites responsible for each behavioral defect, they suggest plausible correlations between the two. In particular, a decrease in the number of trigeminal ganglion neurons could produce sensory defects in the face

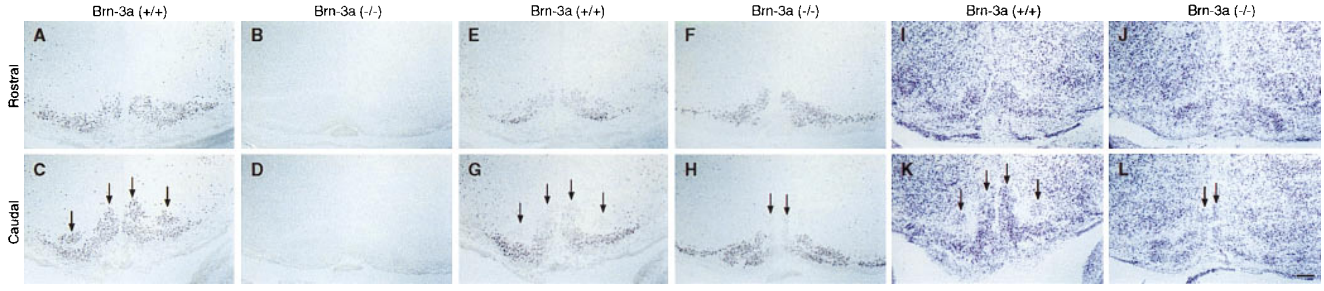

FIG. 8. Inferior olivary nucleus in *Brn-3a* (−/−) mice at e20. For each staining condition, pairs of sections are shown from the rostral and caudal regions of the inferior olivary nucleus. In *Brn-3a* (+/+) mice, the patterns of Brn-3a (*A* and *C*) and Brn-3b (*E* and *G*) immunoreactivity are similar in both rostral and caudal regions of the inferior olivary nucleus, except that Brn-3b immunoreactivity is weak or absent in the dorsal division in the caudal region (vertical arrows in *C* and *G*). In *Brn-3a* (−/−) mice, Brn-3a immunoreactivity is absent as expected (*B* and *D*), and Brn-3b immunoreactivity shows little change (*F* and *H*). Cresyl violet staining shows a diminution in the number of cells in the caudal region of the inferior olivary nucleus (*I–L*). (Bars = 100 μm.)

and mouth that impair the suckling response. With respect to coordination of limb and trunk movement, the observed phenotype could arise from defects in one or more intrinsic spinal reflexes or in any of the pathways that integrate ascending information from the dorsal root ganglia or descending information from the motor cortex or cerebellum. As the red nucleus conveys information from the cerebellum and the cerebral cortex to the spinal cord via the rubrospinal tract and the inferior olivary nucleus integrates sensory information and sends its output to the cerebellar Purkinje cells, defects in these two nuclei could plausibly impair limb and trunk coordination or posture (32). Functional alterations in the dorsal root ganglia related to the loss of *Brn-3b* and *Brn-3c* expression could also play a role in this phenotype.

In the normal mouse retina, trigeminal ganglion, and dorsal root ganglion, the cells that express *Brn-3b* and/or *Brn-3c* form a subset or largely coincide with the cells that express *Brn-3a* (21). In *Brn-3b* (−/−) mice, *Brn-3a* and *Brn-3c* expression is unaltered in the dorsal root and trigeminal ganglia but is diminished in the retina as a consequence of the ≈70% decrease in retinal ganglion cell number (26, 27). By contrast, in *Brn-3a* (−/−) mice, expression of *Brn-3b* and *Brn-3c* is unaffected in the retina but is dramatically reduced in the dorsal root and trigeminal ganglia. We infer, therefore, that in the course of normal development *Brn-3a* expression directly or indirectly leads to the activation of *Brn-3b* and *Brn-3c* in subsets of dorsal root and trigeminal ganglion neurons but does not play a role in their activation in the retina.

In the developing central nervous system, both *Brn-3a* and *Brn-3b* are expressed in subsets of cells in the superior and inferior colliculi, dorsal central gray, and interpeduncular nucleus (Fig. 7). Neither *Brn-3a* (−/−) nor *Brn-3b* (−/−) mutants show obvious defects in the number of neurons in these regions, suggesting that *Brn-3a* and *Brn-3b* play no role in the development of these neurons, that they alter cellular characteristics other than cell number, or that they function redundantly.

Functional Diversification of the *Unc-86*/*Brn-3* Gene Family. The high degree of sequence similarity between the POU domains of *Unc-86* and the *Brn-3* family and the conserved *Brn-3* gene structures suggest that the *Brn-3* genes arose by duplication and divergence of an ancestral *Unc-86*-like gene. As discussed below, the *Unc-86* and *Brn-3* genes also bear intriguing functional similarities as seen in their expression in subsets of neurons and in the phenotypic consequences of their mutation.

In *C. elegans*, *Unc-86* is expressed exclusively in neurons and neuroblasts. Of the 302 neurons in the adult, 57 express *Unc-86*, including sensory neurons, motor neurons, and interneurons (23), and the *Unc-86* phenotype includes defects in mechanosensation, chemotaxis, and egg laying (22, 33). Analysis of *Unc-86* mutants at the single cell level reveals defects both during and following the period of cell proliferation leading to subtle changes in neuronal phenotype, to neuronal loss, and to the generation of supernumerary neurons. Thus *Unc-86* appears to be involved in a variety of developmental decisions that differ depending on the cellular context.

Each member of the *Brn-3* family is expressed in a small subset of neurons in the brainstem and in the auditory (*Brn-3c*), somatosensory (*Brn-3a*, *Brn-3b*, and *Brn-3c*), or visual systems (*Brn-3a*, *Brn-3b*, and *Brn-3c*). Expression in each sensory system is confined to cells close to or at the site of sensory transduction: cochlear and vestibular hair cells, primary somatosensory neurons, and retinal ganglion cells. Interestingly, the phenotypes associated with mutation in each *Brn-3* gene reveal a greater degree of functional specialization than the partially overlapping zones of expression would suggest: the only anatomic defect thus far identified in *Brn-3b* (−/−) mice is a decrease of 70% in retinal ganglion cell number (26, 27); and the only defects apparent in *Brn-3c* (−/−) mice is a loss of vestibular and cochlear hair cells and a secondary degeneration of their associated sensory ganglia (26). As described above, *Brn-3a* (−/−) mice show a decrease in the number of neurons in the trigeminal ganglia but do not show any abnormalities in the retina. This functional diversification of *Brn-3* family members indicates that the expansion and evolution of specialized sensory systems in more complex organisms has been accompanied by a parallel expansion and evolution of genetic regulatory proteins. Thus, these observations suggest that despite the great differences in transduction mechanisms, sensory organ structures, and central information processing of the auditory, somatosensory, and visual systems, there may be fundamental homologies in the genetic regulatory events that control their development.

We thank Drs. Janine Davis, Randall Reed, and Anthony Frankfurter for antibodies and Drs. Randall Reed and King-wai Yau for helpful comments on the manuscript. This work was supported by the National Eye Institute and the Howard Hughes Medical Institute (J.N.), and by the National Institutes of Health and the Robert Welch Foundation (W.H.K.)

1. Herr, W., Sturm, R. A., Clerc, R. G., Corcoran, L. M., Baltimore, D., Sharp, P. A., Ingraham, H. A., Rosenfeld, M. G., Finney, M., Ruvkin, G. & Horvitz, H. R. (1988) *Genes Dev.* **2,** 1513–1516.
2. Wegner, M., Drolet, D. W. & Rosenfeld, M. G. (1993) *Curr. Opin. Cell Biol.* **5,** 488–498.
3. Bodner, M., Castrillo, J.-L., Theill, L. E., Deerinck, T., Ellisman, M. & Karin, M. (1988) *Cell* **55,** 505–518.
4. Ingraham, H. A., Chen, R., Mangalam, H. J., Elsholtz, H. P., Flynn, S. E., Lin, C. R., Simmons, D. M., Swanson, L. & Rosenfeld, M. G. (1988) *Cell* **55,** 519–529.
5. Li, S., Crenshaw, E. B., Rawson, E. J., Simmons, D. M., Swanson, L. W. & Rosenfeld, M. G. (1990) *Nature (London)* **347,** 528–533.
6. Tatsumi, K., Miyai, K., Notomi, T., Kaibe, K., Amino, N., Mizuno, Y. & Kohno, H. (1992) *Nat. Genet.* **1,** 56–58.
7. Radovick, S., Nations, M., Du, Y., Berg, L. A., Weintraub, B. D., Wondisford, F. E. (1992) *Science* **257,** 1115–1118.
8. Pfaffle, R. W., DiMattia, G. E., Parks, J. S., Brown, M. R., Wit, J. M., Jansen, M., Van der Nat, H., Van den Brande, J. L., Rosenfeld, M. G., Ingraham, H. A. (1992) *Science* **257,** 1118–1121.
9. LeMoine, C. & Young, W. S. (1992) *Proc. Natl. Acad. Sci. USA* **89,** 3285–3289.
10. Mathis, J. M., Simmons, D. M., He, X., Swanson, L. W. & Rosenfeld, M. G. (1992) *EMBO J.* **11,** 2551–2561.
11. de Kok, Y. J. M., van der Maarel, S. M., Bitner-Glindzicz, M., Huber, I., Monaco, A. P., Malsolm, S., Pembrey, M. E., Ropers, H.-H. & Cremers, F. P. M. (1995) *Science* **267,** 685–688.
12. Nakai, S. Kawano, H., Yudate, T., Nishi, M., Kuno, J., Nagata, A., Jishage, K., Hamada, H., Fujii, H., Kawamura, K., Shiba, K. & Noda, T. (1995) *Genes Dev.* **9,** 3109–3121.
13. Schonemann, M. D., Ryan, A. K., McEvilly, R. J., O'Connell, S. M., Arias, C. A., Kalla, K. A., Li, P., Sawchenko, P. E. & Rosenfeld, M. G. (1995) *Genes Dev.* **9,** 3122–3135.
14. Finney, M., Ruvkin, G. & Horvitz, H. R. (1988) *Cell* **56,** 757–769.
15. Treacy, M., He, X. & Rosenfeld, M. G. (1991) *Nature (London)* **350,** 577–584.
16. Treacy, M. N., Neilson, L. I., Turner, E. E., He, X. & Rosenfeld, M. G. (1992) *Cell* **68,** 491–505.
17. Xiang, M., Zhou, L., Peng, Y.-W., Eddy, R. L., Shows, T. B. & Nathans, J. (1993) *Neuron* **11,** 689–701.
18. Theil, T., McLean-Hunter, S., Zornig, M. & Moroy, T. (1993) *Nucleic Acids Res.* **21,** 5921–5929.
19. Gerrero, M. R., McEvilly, R., Turner, E., Lin, C. R., O'Connell, S., Jenne, K. J., Hobbs, M. V. & Rosenfeld, M. G. (1993) *Proc. Natl. Acad. Sci. USA* **90,** 10841–10845.
20. Turner, E. E., Jenne, K. J. & Rosenfeld, M. G. (1994) *Neuron* **12,** 205–218.
21. Xiang, M., Zhou, L., Macke, J. P., Yoshioka, T., Hendry, S. H. C., Eddy, R. L., Shows, T. B. & Nathans, J. (1995) *J. Neurosci.* **15,** 4762–4785.
22. Chalfie, M., Horvitz, H. R. & Sulston, J. E. (1981) *Cell* **24,** 59–69.
23. Finney, M. & Ruvkin, G. (1990) *Cell* **63,** 895–905.
24. Ninkina, N. N., Stevens, G. E. M., Wood, J. N. & Richardson, W. D. (1993) *Nucleic Acids Res.* **21,** 3175–3182.
25. Fedtsova, N. G. & Turner, E. R. (1995) *Mech. Dev.* **53,** 291–304.
26. Erkman, L., McEvilly, R. J., Luo, L., Ryan, A. K., Hooshmand, F., O'Connell, S. M., Keithley, E. M., Rapaport, D. H., Ryan, A. F. & Rosenfeld, M. G. (1996) *Nature (London)* **381,** 603–606.
27. Gan, L., Xiang, M., Zhou, L., Wagner, D. S., Klein, W. H. & Nathans, J. (1996) *Proc. Natl. Acad. Sci. USA* **93,** 3920–3925.
28. Davis, J. A. & Reed, R. R. (1996) *J. Neurosci.,* **16,** 5082–5094.
29. Moody, S. A., Quigg, M. S. & Frankfurter, A. (1996) *J. Comp. Neurol.* **279,** 567–580.
30. Karnovsky, M. J. & Roots, L. (1964) *J. Histochem. Cytochem.* **12,** 219–221.
31. Munger, B. L. & Ide, C. (1988) *Arch. Histol. Cytol.* **51,** 1–34.
32. Paxinos, G. (1995) *The Rat Nervous System* (Academic, San Diego).
33. Hodgkin, J., Horvitz, H. R. & Brenner, S. (1979) *Genetics* **91,** 67–94.